

EFFECTS OF COMPACTION ON SMALL STRAIN YOUNG'S MODULI OF GRAVEL BY DYNAMIC AND STATIC MEASUREMENTS

Sajjad MAQBOOL¹, Junichi KOSEKI² and Takeshi SATO³

ABSTRACT: The effect of compaction on small strain Young's moduli was investigated by performing triaxial compression tests using medium scale triaxial and large scale true triaxial apparatuses. Static and dynamic Young's moduli were evaluated based on results from small cyclic loading and wave velocity measurements. Two series of tests were conducted using Chiba gravel as testing material. In the first series of tests, particles having a diameter larger than 10.5 mm were removed and cylindrical specimens of 10 cm (diameter) x 20 cm (height) having dry densities of 1.76 g/cm³ and 2.00 g/cm³ were prepared. In the second series of experiments, the original gradation with $D_{max} = 38$ mm was used to prepare prismatic specimens of 23.5 cm x 23.5 cm x 50 cm having dry densities in the range of 1.92 - 2.15 g/cm³. Comparison between statically and dynamically measured Young's moduli was made between test results on these specimens with different dry densities and gradations.

Key Words: Compaction, gravel, local deformation transducer, wave velocity, accelerometers, Young's modulus.

INTRODUCTION

Construction of very large embankments for highway projects, railway track for bullet train, large industrial complexes on extensive land reclamation fills and coastal deposits as well as increasing concern about liquefaction due to earthquake loads have caused very high compaction requirements for gravel material. Loose granular deposits are known to undergo large settlements when subjected to vibration arising from machinery, traffic loads and earthquakes. Under static loading, non-uniform density variations can cause relatively large differential settlement even though the total settlement of the structures on granular material is small. To avoid structural damage due to settlement, it is necessary to compact loose granular material prior to construction.

However, these days with the development of new techniques, it has become possible to obtain very high dry density in the field, while it has been observed that under working loads, the strain levels within these highly dense deposits as well as in well-designed geotechnical structures are relatively small (Tatsuoka & Kohata, 1995).

In soil mechanics, it is normally assumed that the ground material is a continuum, and that the behavior is linear and recoverable within a very small strain range i.e. lesser than 10⁻³ % (Tatsuoka & Shibuya, 1992). For the measurement of this "elastic" strain range, the experimental devices have to be very precise and accurate. In this study, very small unloading/reloading cycles were applied at some stress levels, and strains were measured locally using local deformation transducers within a

¹ Doctoral Candidate, Civil Engineering Department, The University of Tokyo

² Professor, Institute of Industrial Science, The University of Tokyo

³ Research Associate, Institute of Industrial Science, The University of Tokyo

very small strain range at the specimen sides. This method is herein called as “static”. For the “dynamic” measurement in this study, by triggering with pulse wave at some stress levels, the velocity of vertically transmitting compression waves was evaluated from the time difference between the input and output signals.

In the past, dynamic wave measurements, based on the cross-hole and down-hole methods, have been used for a long time in real construction sites (Stokoe & Hoar, 1978). Recently measurement of wave velocities in the laboratory has also become popular, and researchers have recognized that “static” and “dynamic” properties are no more different from each other (Woods, 1991). Precise static small strain measurements in the laboratory tests have bridged the gap of strain levels between “static” and “dynamic” behavior (Tatsuoka and Shibuya, 1992). However, following the pioneer work by Tanaka et al. (2000), Anhdan and Koseki (2002) found that the difference of static and dynamic properties is not only caused by strain level but also by some other factors like grain size and wavelength. In their preliminary conclusion, the bigger the particle is, the larger the dynamic Young’s modulus becomes as compared with the static one. In this paper, not only the grain size but also the dry densities are varied to check the effect of compaction on Young’s moduli by “dynamic” and “static” measurements.

TESTING MATERIAL, EQUIPMENT AND TEST PROCEDURES

Specimen preparation

In this study two series of tests were conducted.

In the first series of tests, medium scale triaxial apparatus was employed. The testing material, as shown in **Figure 1**, was Chiba gravel-1 ($D_{max}=10.5$ mm, $D_{50}=3$ mm and $U_c=16$) that was prepared from the original Chiba gravel (Chiba gravel-2 in **Figure 1**) after removing particles having a diameter larger than 10.5mm. The specimen, as shown in **Figure 2**, was cylindrical in shape with dimensions of 10 cm in diameter and 20 cm in height. To measure the vertical stress, σ_1 , a load cell is located just above the top cap inside the triaxial cell in order to eliminate the effects of piston friction (Tatsuoka, 1988). The vertical strain ϵ_1 was measured not only with the external displacement transducer but also with a pair of vertical local deformation transducers (LDTs) (Goto et al, 1991), located each on opposite side surfaces of the specimen. The horizontal stress σ_3 was applied through the water in the cell, which was measured with a high capacity differential pressure transducer (HCDPT).

In this series of tests, two specimens named as G-2 & G-3,

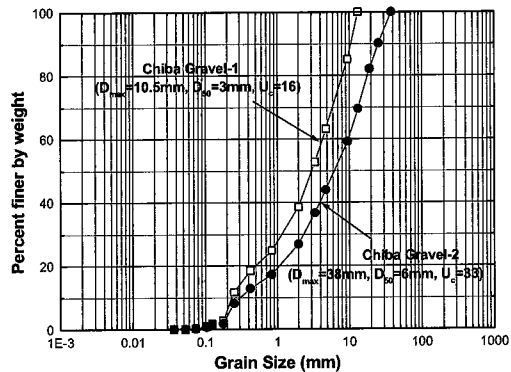


Figure 1. Grain size distribution curve of the test material

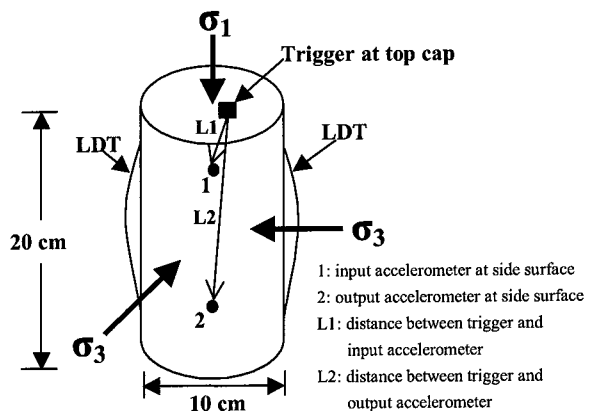


Figure 2. Positioning of LDTs, trigger and accelerometers on medium scale cylindrical specimen

were prepared in five layers, and their compaction was made manually by using a compactor having a mass of 5 kg with pre-calibrated number of blows under a free-falling height of 0.455 m that was applied on each layer for achieving the required dry density of 1.92 g/cm³ and 2.00 g/cm³. The membrane used in these tests was 0.5 mm thick. The specimens were partially saturated with water content kept at 5.5%.

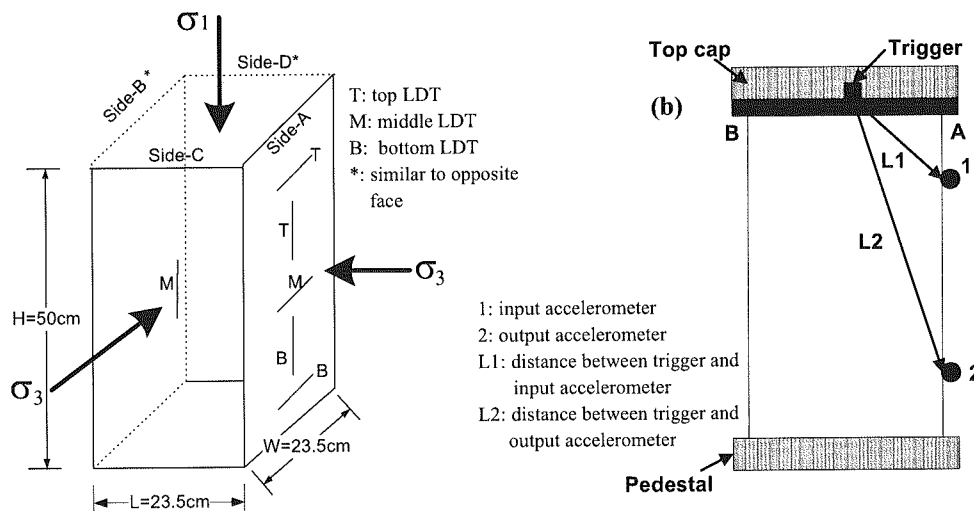


Figure 3. Large scale triaxial specimen;(a) Positioning of LDTs & (b) Location of trigger and accelerometers

In the second series of tests Chiba gravel-2 ($D_{\max}=38\text{ mm}$, $D_{50}=6\text{ mm}$ and $U_c=33$) as shown in **Figure 1**, was used as the test material. Due to larger particle size of this material, a large-scale true triaxial apparatus (Sato et al., 2001) was employed. With this apparatus, all three-principle stresses (σ_1 , σ_2 , σ_3) can be controlled independently, though in this study it was used just as a triaxial apparatus. The specimen, as shown in **Figure 3a**, was rectangular prismatic with dimensions of 50 cm high and 23.5 cm times 23.5 cm in cross-section. To measure the vertical stress σ_1 , a load cell is located just above the top cap inside the triaxial cell. The vertical strain ϵ_1 was measured not only externally but also locally with three pairs of vertical local deformation transducers (LDTs). Minor principle stress σ_3 was applied through the cell pressure, which was measured with high capacity differential pressure transducer (HCDPT). The corresponding horizontal strain ϵ_3 was measured with three pairs of horizontal local deformation transducers (LDTs).

In the second series of tests, three partially saturated specimens, named as TC-1, TC-2 & TC-3, were prepared by employing manual impact loading using steel tamper at water content of 5.5%. Each specimen was prepared in 10-12 layers of equal thickness to obtain overall dry densities in the range of 1.92-2.15 g/cm³. The thickness of each layer was controlled by applying a pre-calibrated number of blows with the tamper mass of 12 kg from a fixed free-falling height of 0.545 m. Using this technique of compaction, it became possible to obtain higher dry density even up to 2.15 g/cm³ along with quantitative measurement of the compaction energy. It required the unit compaction energy of 766 and 8084 kJ/m³ to achieve the dry density of 1.92 and 2.15 g/cm³, respectively.

Generating dynamic waves

In order to generate dynamic waves, as shown in **Figure 4a**, a special type of wave source (denoted as trigger) was employed. It is a multi-layered piezoelectric actuator made of ceramics (dimensions of 10 mm x 10 mm x 20 mm, mass of 35 gram and natural frequency of 69 kHz, the commercial name is AE 1010D16 of TOKIN company) and a thick steel bar that was bent in a U shape. The actuator was driven by inputting an electric signal of +25 volt in a form of pulse. The mass of each steel bar is 60 grams, and such a large mass was required to provide the reaction force against the dynamic

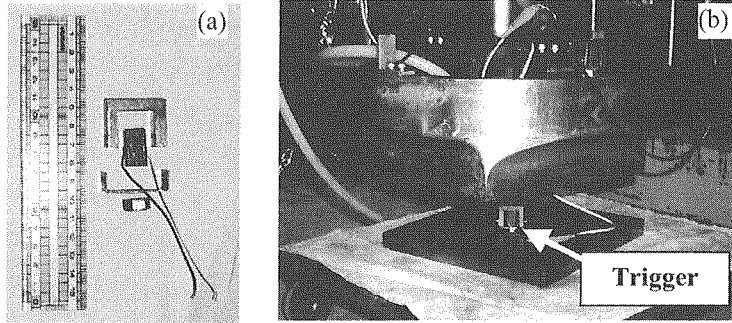


Figure 4. (a) Components of a trigger & (b) Position of trigger inside the top cap of large-scale true triaxial apparatus

excitation by the piezoelectric actuator. The actuator was put inside the U-shaped steel bar, and they were covered by another steel plate. To generate the vertical compression wave that transmits from the top to the bottom of the specimen, the trigger was glued above the top cap close to the center in the case of the medium scale triaxial apparatus (**Figure 2**). In the case of the large-scale true triaxial apparatus, as shown in **Figures 3b and 4b**, the trigger was glued inside the top cap.

Receiving dynamic waves

As shown in **Figure 5**, two types of piezoelectric accelerometers were employed to receive dynamic waves. The type-1 accelerometers were cylindrical in shape with diameter of 3.6 mm, height of 3 mm, mass of 0.16 gram and natural frequency of 60 kHz (the commercial name is Yamco10SW of YAMAICHI DENKI company) and these were used for the medium scale specimen. The output voltage of these accelerometers was sometimes significantly low, therefore while testing on large-scale specimens, the type-2 accelerometers were introduced. These were box-shaped with sizes of 4 mm x 4 mm x 13 mm, mass of 1.3 gram and natural frequency of 4 kHz (the commercial name is Yamco111BW of YAMAICHI DENKI company) and the output voltage was always high enough.

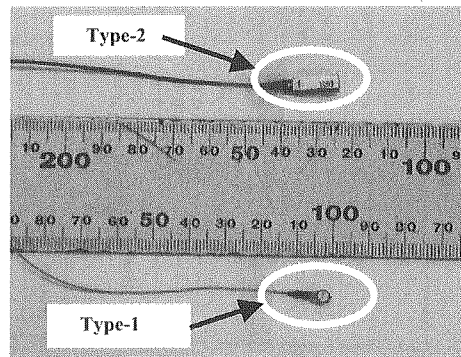


Figure 5. Accelerometers used for dynamic measurement

For each test in both series of experiments, the testing conditions are given in **Table 1**.

Table 1. Testing conditions during the first and second series experiments

Test	Apparatus	Material	Specimen size	Dry density (g/cm ³)	Accelerometers
G-2	Medium Scale Triaxial	Chiba gravel-1	10cm(dia) x 20 cm (height)	1.76	Type-1 (cylindrical)
G-3				2.00	
TC-1	Large Scale True Triaxial	Chiba gravel-2	23.5x23.5x50 cm ³	1.92	Type-2 (box type)
TC-2				2.08	
TC-3				2.15	

Evaluating vertical Young's modulus

To evaluate quasi-elastic vertical Young's modulus based on static measurements, at some stress levels, very small unloading/ reloading cycles were applied on the specimen in the vertical direction. Existing data on the deformation properties from cyclic loading tests on dense gravelly soils reported in the literature showed that the behavior at strains lesser than about 0.001% is nearly elastic (Jiang et al. 1997). Typical stress-strain relationship during a small vertical loading cycle is shown in **Figure 6**. The increments of the vertical strain and stress were detected with the local deformation transducers (LDTs) and the internal load cell, respectively. Stress-strain relationships were fitted by a straight line, and the quasi-elastic vertical Young's modulus E_s was evaluated from the slope of the line.

For dynamic measurements, in order to receive a clear signal, AnhDan et al. (2002) suggested to use continuous sinusoidal input for trigger excitation while testing on gravel specimens. In their approach it is sometimes difficult to decide the arrival of the output signal corresponding to the arrival of the respective input signal. So in this study by triggering vertically with a single pulse wave at some stress levels, an appropriate wave velocity was evaluated. As the top cap touched the whole cross-section of the specimen that was with free side boundaries, we assumed that unconstrained compression waves were generated. Its wave velocity V_p is directly related to the small-strain vertical Young's modulus, E_d , of the material by the dynamic measurement as:

$$E_d = \rho V_p^2 \quad (1)$$

where ρ is the mass density of the specimen, and the compression wave velocity V_p was calculated by

$$V_p = L/t \quad (2)$$

Here t is the travel time of the wave to cover the distance L . The distance L was computed by using the following equations considering the trigger as a point source to generate the compression waves as shown in **Figures 2 & 3b**.

$$L = L_2 - L_1 \quad (3)$$

$$L_2 = \sqrt{(X_2 - X_0)^2 + (Y_2 - Y_0)^2 + (Z_2 - Z_0)^2} \quad (4)$$

$$L_1 = \sqrt{(X_1 - X_0)^2 + (Y_1 - Y_0)^2 + (Z_1 - Z_0)^2} \quad (5)$$

while X_0, Y_0, Z_0 : coordinates of the trigger

X_1, Y_1, Z_1 : coordinates of the location of the input accelerometer "1"

X_2, Y_2, Z_2 : coordinates of the location of the output accelerometer "2"

All the above parameters could be calculated or measured easily except for the travel time "t". In many previous researches, a variety of methods to obtain the "correct" travel time have been employed. For example, AnhDan et al. (2002) used the peak-to-peak travel time, while Jovicic et al. (1996) have recommended using the first arrival of the wave. Other researchers have suggested

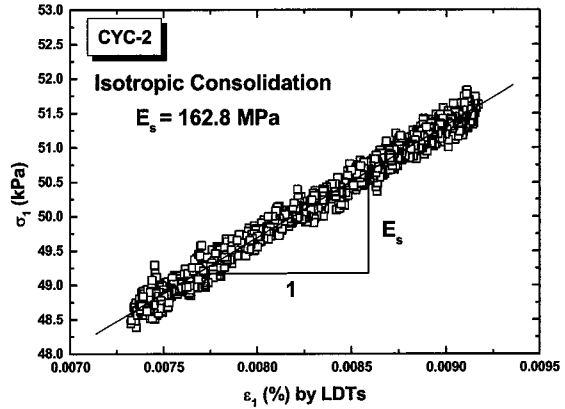


Figure 6. Typical stress-strain relationship during a small vertical loading cycle

estimation of the travel time from several characteristic points, such as the first rising points, first peaks & first zero-crossing points in the input and output signals. There are also some researchers who have suggested to conduct analysis in the frequency domain to determine the phase angle either indirectly (e.g. Viggiani & Atkinson, 1995) or directly using phase-sensitive detection techniques (e.g. Blewett et al., 1999).

Travel time computation

In this study the wave signals were recorded at two different levels over the specimen using the input and output accelerometers named as “1” & “2” respectively (Figures 2 & 3b). Four different techniques were employed to compute the travel time and compared.

In the first technique as shown in Figure 7 a, “t” was determined using the first peaks of input and output waves. It will be called “peak to peak” travel time technique denoted as “t_{pk}”. In this technique, the observer has to decide the correct peak point. In case of noise-free signal records, the error on decision of “correct peak” are lesser than in case of noisy signal records. The authors recommend using this technique for the determination of correct travel time when the data is almost noise free.

In the second technique, as shown in Figure 7a, “t” was computed from the first rising point of the first input wave to the first rising point of the first output wave. It will be called as “first rise to first rise” technique denoted as “t_{rise}”. In this method, a problem lies with the decision of first rising point in both signal records. It may depend on observer’s judgment to decide the correct rising point. After comparing a number of wave signal records obtained in the second series of tests, it was found that t_{rise} was in general by about 5% larger than t_{pk}.

The third technique employed in this study is to use cross-correlation. For this technique, a computer program in PERL language was developed to compute the cross-correlation between the input wave data and the output wave data. The cross-correlation function CC_{xy}(t) is a measure of the degree of correlation of the input and output two signals, X(T) and Y(T), respectively. The analytical expression of the cross-correlation function is,

$$CC_{xy}(t) = \frac{1}{T_r} \int_{T_r} X(T)Y(T+t)dT \quad (6)$$

where T_r is the length of the time records to be matched, and t is the time lag between the signals.

As a first attempt only the first full cycle of the input wave was matched with the full length of the output wave by giving an increment of 10μs (equal to data interval) for the time lag, as shown in Figure 7b. The travel time of the wave denoted as “t_{xcorr}” was computed by taking time difference from the starting point of the input wave to the “largest peak” of the cross-correlation. In general the difference between t_{pk} and t_{xcorr} was within 3%.

The last technique employed also the cross-correlation. In this technique, as shown in Figure 7c, instead of matching the first full cycle of the input wave, the first half cycle was matched with the full length of output wave to obtain the cross-correlation. The reason for taking just the first half cycle input wave is to avoid excessive effects of the second half cycle that had a larger amplitude than the first one. The travel time obtained by this technique is denoted as “t_{halfxcorr}”. In general the value of t_{halfxcorr} was found almost the same as t_{pk}.

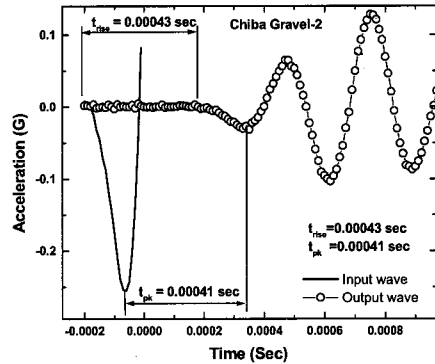


Figure 7. Measurement of travel time “t” of wave using; (a) first rise and first peak techniques (to continue)

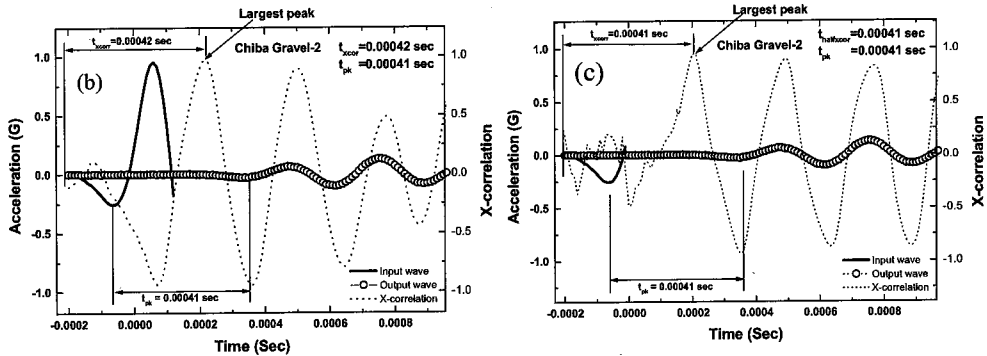


Figure 7 (continued). Measurement of travel time “t” of wave using; (b) full input wave cycle cross-correlation technique & (c) half input wave cycle cross-correlation technique

Based on the above comparison, it was found that, if the signal record is noise free, then “ t_{pk} ” is easily employed, while in case of slightly noisy data “ $t_{halfcorr}$ ” should be used to compute travel time of wave. In the following test results, “ t_{pk} ” was used to compute the travel time.

TEST RESULTS AND DISCUSSION

Vertical Young’s moduli of Chiba gravel-1

The specimens were subjected to isotropic consolidation. At various stress levels, compression waves were generated while keeping the stress states constant, followed by application of small vertical unload-reload cycles in order to evaluate the quasi-elastic Young’s moduli. In all tests, as typically shown in **Figure 6**, the strain amplitude during small unloading/reloading cycles was around 0.001%, which is considered to be within the elastic limit. Values of the vertical Young’s moduli of Chiba gravel-1, evaluated by the static and dynamic measurements are compared in **Figure 8**. In the first test on specimen G-2 ($\rho_d = 1.76 \text{ g/cm}^3$), it was observed that the dynamic Young’s moduli were almost twice as large as the static Young’s moduli at all stress levels. On the other hand, in the second test on a denser specimen (G-3, $\rho_d = 2.00 \text{ g/cm}^3$), the values of the static Young’s moduli increased by a factor of about two in G-2. However, the values of the dynamic Young’s moduli in G-3 were almost similar to those in G-2.

From these observations, it was found that by the increase of dry density from 1.76 g/cm^3 to 2.00 g/cm^3 , the difference between the static and dynamic Young’s moduli was reduced. In order to confirm this behavior, the second series of tests was conducted as given in the following section.

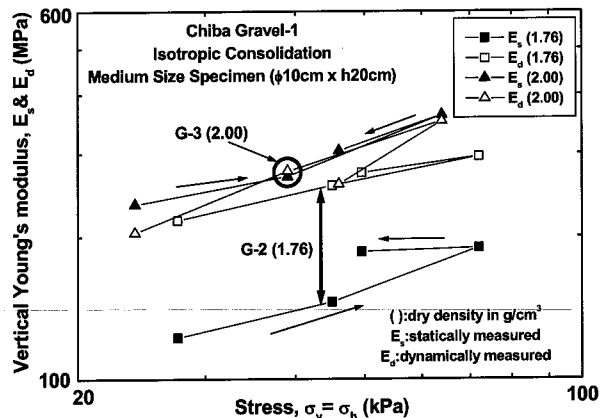


Figure 8. Comparison of vertical Young’s moduli during isotropic consolidation for Chiba gravel-1 ($D_{max} = 10.5 \text{ mm}$)

Vertical Young's moduli of Chiba gravel-2

The second series of tests on Chiba gravel-2 was conducted using large-scale prismatic specimens. Static and dynamic measurements were made in a similar manner as were employed in the first series of tests. Among three specimens as shown in **Figure 9**, the first one, named TC-1, was the loosest one having dry density of 1.92 g/cm^3 . With this specimen, the difference between the static and dynamic Young's moduli was the largest as compared to the other two test results. In the second test, TC-2 ($\rho_d = 2.08 \text{ g/cm}^3$), the values of the static and dynamic Young's moduli were larger than those in TC-1 though the difference between the static and dynamic Young's moduli became smaller than that in TC-1. The third test TC-3 ($\rho_d = 2.15 \text{ g/cm}^3$) showed some different behavior. The values of the static Young's moduli were larger while the values of the dynamic Young's moduli were lower than the other two test results. It was found that the difference between the static and dynamic Young's moduli was reduced by the increase in the dry density of the specimens. Such behavior of these test results confirmed the behavior observed in the first series of tests as mentioned before.

The reason for the above behavior would be that in the dynamic measurement unlike the static measurement the wave does not reflect the overall cross-sectional property of the specimen but travels through the shortest path made by interlocking of bigger particles, resulting into larger Young's moduli as compared to those by the static measurement. The difference in the Young's moduli would increase with the decrease in the dry density, since looser specimens would have larger structural or microscopic heterogeneity than denser ones.

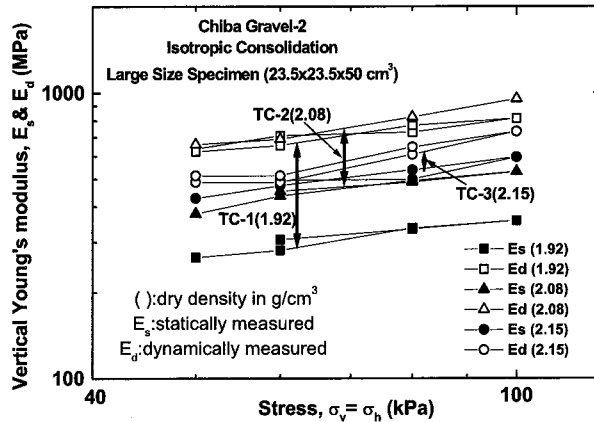


Figure 9. Comparison of vertical Young's moduli during isotropic consolidation for Chiba gravel-2 ($D_{max} = 38 \text{ mm}$)

Effects of compaction on ratio of static and dynamic wave velocity

It would be natural to assume that different elastic moduli between static and dynamic measurements are affected by the different physical properties of gravelly soils, such as grain size, uniformity coefficient, dry density and wavelength employed in the dynamic measurement. The larger grain size and larger uniformity coefficient of soil would lead to larger structural or microscopic heterogeneity inside the specimen. Tanaka et al. (2000) and AnhDan et al. (2002) reported that the difference between the static and dynamic measurements in terms of wave velocities was affected by the values of $D_{50}/(\lambda/2)$, where λ is the wavelength in the dynamic measurement. In this study, the results obtained from both series of tests having different dry densities and specimen size were converted to V_{cyc}/V_{sv} where V_{cyc} is the wave velocity converted from the static Young's moduli method and V_{sv} is the wave velocity employed in the dynamic measurement. The value of λ was computed using the same definition as used by Tanaka et al. (2000). The test results from this study that are measured at confining stress of 50kPa during isotropic consolidation are shown in **Figure 10**. At relatively low dry density, the relationships between V_{cyc}/V_{sv} and $D_{50}/(\lambda/2)$ observed in this study were consistent with those from previous studies. It is observed, however, that $D_{50}/(\lambda/2)$ is not the only parameter to affect the values of V_{cyc}/V_{sv} , but the dry density is also an important factor. Both series of tests on Chiba gravel-1 & Chiba gravel-2 specimens showed an increasing trend of V_{cyc}/V_{sv} with the increase in the dry density. It can be concluded that specimens though having similar values of $D_{50}/(\lambda/2)$ can have different V_{cyc}/V_{sv} values depending on their dry density.

During large earthquakes, the predominant frequency of earthquake motions in the subsurface soils is around 1-2 Hz. At this frequency even for big particle sizes like the gravel tested in the

present study, the values of $D_{50}/(\lambda/2)$ would be at largest 0.0005 when effects of non-linearity are neglected. If we assume that the tendency of the difference between the static and dynamic values can be extrapolated from the results above, the difference in the wave velocities between the two methods will be negligibly small, suggesting that the small strain deformation properties evaluated based on the static methods can be employed in the seismic response analysis. The difference will be even very small for compacted ground as compared to the loose ground. On the other hand, if these properties are evaluated based on in-situ dynamic measurement using shorter wavelengths, due corrections should be made.

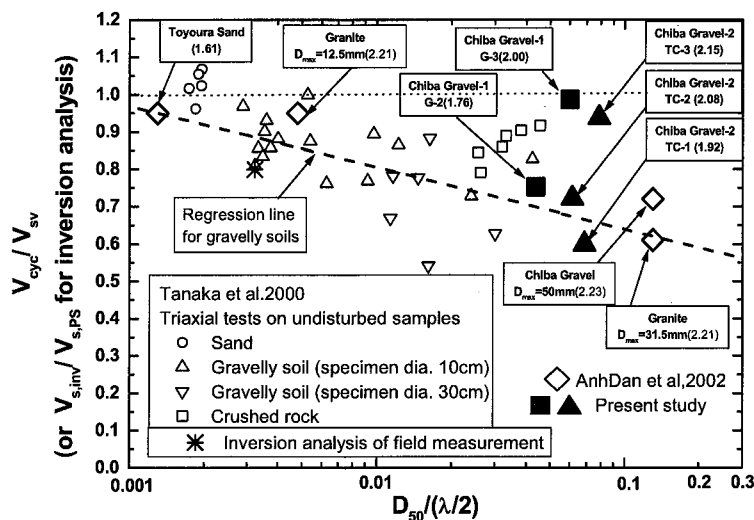


Figure 10. Effects of particle size, wave length and dry density (modified from Tanaka et al. 2000 & AnhDan et al. 2002)

CONCLUSIONS

The following conclusions can be drawn from the test results presented in this paper:

- 1- The technique using cross-correlation method by considering “first half cycle of input wave” and full length of output wave signal was found consistent with the peak-to-peak technique for the determination of travel time during wave velocity measurement.
- 2- The difference between the static and dynamic vertical Young’s moduli decreased with the increase in the dry density of compacted gravel. This behavior was observed not only in the medium scale cylindrical specimens but also in the large-scale prismatic specimens.
- 3- At relatively low dry density, the relationships between V_{cyc}/V_{sv} and $D_{50}/(\lambda/2)$ observed in this study were consistent with those from previous studies.

ACKNOWLEDGEMENTS

The authors want to express deep gratitude to Mr. Shamas-ul-Islam Bajwa for the help provided regarding development of a computer program for cross-correlation techniques used to compute the travel time of wave. Special acknowledgement to the Ministry of Science, Culture and Education, Japan for providing the first author with financial assistance for his studies in Japan.

REFERENCES

- AnhDan, L.Q., Koseki, J. and Sato, T. (2001). "Comparison of Young's moduli of dense sand measured by dynamic and static methods." Proceedings of the Thirty-Sixth Japan National Conference on Geotechnical Engineering, Tokushima, Vol.1, pp.447-448.
- AnhDan, L.Q., Koseki, J. and Sato, T. (2002). "Comparison of Young's moduli of dense sand and gravel measured by dynamic and static methods." Geotechnical Testing Journal, Vol.25, No.4, pp.349-368.
- AnhDan, L.Q. and Koseki, J. (2002). "Effects of particle sizes on dynamic and static small strain deformation properties." Proceedings of the Thirty-Seventh Japan National Conference on Geotechnical Engineering, Osaka, Japan, Vol.1, pp.603-604.
- Blewett, J., Blewett, I.J. and Woodward, P.K. (1999). "Measurement of shear-wave velocity using phase-sensitive detection techniques, Canadian Geotechnical Journal, No.36, pp.934-939.
- Goto, S., Tatsuoka, F., Shibuya, S., Kim, Y.S. and Sato, T. (1991). "A simple gauge for local small strain measurements in the Laboratory." Soils and Foundations, No.1, Vol.31, pp.169-180.
- Jiang, G.L., Tatsuoka, F., Flora, A. and Koseki, J. (1997). "Inherent and stress-state-induced anisotropy in very small strain stiffness of a sandy gravel." Geotechnique, Vol.47, No.3, pp.509-521.
- Jovicic, V., Coop, M.R., and Simic, M. (1996). "Objective criteria for determining G_{max} from bender element tests." Geotechnique, Vol.46, No.2, pp.357-362.
- Sato, T., AnhDan, L.Q. and Koseki, J. (2001). "Development of true triaxial testing system for large scale apparatus." Proceedings of the Thirty-Sixth Japan National Conference on Geotechnical Engineering, Tokushima, Vol.1, pp.545-546 (in Japanese).
- Stokoe, K.H., II and Hoar, R. J. (1978). "Field measurement of shear wave velocity by crosshole and downhole seismic methods." Proceedings of the Conference on Dynamic Methods in Soil and Rock Mechanics, Karlsruhe, Germany, Vol.III, pp.115-137.
- Tanaka, Y., Kudo, K., Nishi, K., Okamoto, T., Kataoka, T. and Ueshima, T. (2000). "Small strain characteristics of soils in Hualien, Taiwan." Soils and Foundations, Vol.40, No.3, pp.111-125.
- Tatsuoka, F. (1988). "Some recent developments in triaxial testing systems for cohesionless soils." Advanced Triaxial Testing of Soils and Rock, STP 977, ASTM, Philadelphia, pp.7-67.
- Tatsuoka, F. and Kohata, Y. (1995). "Stiffness of hard soils and soft rocks in engineering applications." Proceedings of International Symposium on Pre-failure Deformation of Geomaterials, Vol.2, pp.947-1066.
- Tatsuoka, F. and Shibuya, S. (1992). "Deformation characteristics of soils and rocks from field and laboratory tests." Proc. of 9th Asian Regional Conference of SMFE, Bangkok, Vol. 2, pp.101-170.
- Viggiani, G. and Atkinson, J.H. (1995). "Interpretation of bender element tests." Geotechnique, Vol.45, No.1, pp.149-154.
- Woods, R.D. (1991). "Field and laboratory determination of soil properties at low and high strains." Proc. of 2nd International Conference on Recent Advances in Geotechnical Earthquake Engineering and Soil Dynamics, pp.1727-1741.